ATLAS Note ?
27 Maio 1996

ϕ-scan with pions and muons - Analysis of TILECAL test beam data

P. Amaral, J. Carvalho, F. Colaço, A. Gomes, A. Henriques, A. Maio, A. Onofre, H. Wolters
LIP (Univ. Lisbon, Univ. Coimbra, U.C. Fig. Foz), Portugal

Abstract

The TILECAL 5 prototype modules were exposed to particle beams at the CERN SPS beam. The uniformity of the response to muons and pions with energies from 20 to 300 GeV for $\theta = 10°$ has been studied as a function of the vertical displacement y (phi scan) between 2 modules. The signal response has a good uniformity both for pions and muons with a sigma of 2.0% and 2.4% respectively. A decrease of the signal is observed in the interface between the 2 modules ("crack"). This is a limited region of about 5 mm where the signal response decreases by about 7% for pions and 60% for muons. The pion energy resolution has a negligible degradation in the crack region with respect to the other impact point positions. A scan with muons at $\theta = 90°$ (modules lateral face) allowed to study the direct fibre response and to check the crack dimension.

Contents

1 Introduction

This report presents the results of an analysis of the TILECAL test beam data recorded during the May 95 data taking period. The analysis concerns the detector ϕ-scan, with 20, 50, 100, 180 and 300 GeV pions and 150 GeV muons, in a scan between 2 modules, from the center of module 3 to the center of module 4. This corresponds to a scan along 20 cm in the entrance face of the calorimeter ($\phi = 0.56^o$ corresponds to a vertical displacement of 1 cm in y). The response uniformity for muons and pions and the energy resolution for pions were measured. It was studied the effect in the signal response of the tile non uniformity using new tile masking and tile/fibre coupling geometry in modules 3 and 4. The angle θ between beam and the modules front plate was 10°. Muons were also used, with an angle $\theta = 90^\circ$, for a vertical scan across the 2 modules to test the "crack" dimensions along the radial dimension and the direct fibre response.

2 Test Beam Setup and Data Selection

The data discussed in this paper were taken with a calorimeter prototype consisting of five prototype modules, each spanning $2\pi/64$ in azimuth [1, 2], with a front face of 100×20 cm^2. The radial depth is 180 cm, starting at an inner radius of 200 cm up to an outer radius of 380 cm corresponding to 8.9 interaction lengths (λ) at $\eta = 0$ or to 80.5 radiation lengths (X_0).

The Tile calorimeter uses steel as absorber and scintillator plates, read out by wavelength-shifting fibres, as the sampling material. An innovative feature of this design is the orientation of the tiles which are placed parallel to the $\eta = 0$ plane and staggered in depth. Fibres running radially collect light from the tiles at both of their open edges. Readout cells are then defined by grouping together a set of fibres into a photomultiplier (PMT). Thus each calorimeter cell is read out by 2 PMTs. The calorimeter is radially segmented into four depth segments (corresponding to 1.5, 2, 2.5 and 3 λ at η=0). The transverse segmentation is $\Delta\eta \times \Delta\phi \simeq 0.1 \times 0.1$; it was designed with a full projective geometry in azimuth but not in polar angle. The gain of the PMT's was set to deliver $\simeq$ 6 pC/GeV. The high voltage value of each PMT was adjusted by running a radioactive source through each scintillating tile. The current induced in the PMT is proportional to the PMT gain and to the photoelectron yield of the calorimeter for the scintillation light induced by the source. A pulsed laser, illuminating each PMT by means of clear fibres, has been used to monitor the calorimeter response independently of gain drift.

The five Tile calorimeter modules, stacked along the azimuthal (ϕ) direction, were mounted on a scanning table allowing precise positioning of the impact point on the calorimeter front

face z, and of the beam angles θ, ϕ to each module axis. The geometry of the modules and the coordinate axis used are shown in fig. 1

Beam chambers and beam defining counters were placed upstream of the scanning table. Two scintillator walls, each with a surface of about 1 m^2, were added to one side and to the back of the calorimeter to measure the lateral and longitudinal leakage of the hadronic showers.

The energy of the beam (pions, electrons and muons) was changed from 20 to 300 GeV.

3 Muon response

The uniformity in the y vertical direction (ϕ scan) has been studied using 150 GeV muons at $\theta = 10^o$. Fig. 2 shows the signals in the modules below and above the interface between them (the "crack") as a function of the vertical displacement y ($\phi = 0.56^o$ corresponds to a vertical displacement of 1 cm in y). The sum of the signal of the two modules is also shown. Signals were normalized to the signal at the centre of module 3. The response is the most probable value from a profile histogram.

The y coordinate is measured from the crack, in a plane perpendicular to the crack plane. A drop in the signal of about 60% was measured at y = 0 cm. This crack is mainly due to the space needed to extract the fibres to the PMTs, and consequently less amount of scintillator tile, reducing the sampling fraction. In Fig. 2 the distribution of the normalized signals is also shown together with a Gaussian fit with $\sigma = 2.4\%$. Outside the crack region a rather uniform response over the full module surface is observed. A non-uniform response observed in the past was eliminated in the present prototypes by means of a better tile masking and tile/fibre coupling geometry [3]. The muon signal uniformity in the ϕ direction is shown in fig. 3 for each of the four longitudinal compartments for the PMTs of module 3 and 4, separately for the PMTs which readout the fibres near the crack, far from the crack, and for all the PMTs of these modules. In all depths a drop of the signal is observed due to the lack of scintillator in the crack region and an increased probability of traversing the air gap, partially cancelled by the light production in the fibres, the signal being reduced to 47%, 56%, 59% and 65%, respectively for S1 to S4. This difference is due to the different amount of fibre material traversed by muons. In sampling 1 the drop is smallest because the fibre length is the largest ($\sim 2.2m$). In samplings 2, 3 and 4 the fibre length is about $1.9m$, $1.5m$ and $1m$, respectively [4].

4 Pion Response

The Tile calorimeter prototype was exposed to pions with energies between 20 to 300 GeV and the angle of incidence $\theta = 10°$. Large vertical (y) and horizontal (z) grid scans were performed with 180 GeV pions.

Fig. 4a shows, as a function of y, the signal in the module on one side (module 3) and on the other side (module 4) of the crack, as well as the sum, normalized to the signal at the center of module 3. The y coordinate is measured from the crack, in a line perpendicular to the crack plane, extrapolated to the radial depth of maximum energy deposition (depth=65 cm). This was done using the relation

$$y = ybeam * \frac{265}{200} + (ycha2 - ycha1) * \frac{3840}{2262} + ycha2 \quad (cm) \quad .$$

$ybeam$ is the nominal beam y impact position and $ycha1(ycha2)$ is the y coordinate as measured by the wire chamber 1(2). Each point in Fig. 4 represents the sum of runs taken at the corresponding y bin, for the z interval from -20 cm to 0 cm (integrated over z). For each point

the average energy deposition is the mean value of a profile histogram. In the same figure it is also shown the same plot done using the geometric mean of the two PMTs which readout each cell instead of just the linear sum. The results are very similar. The crack is visible as a small drop of about 7% in the signal at $y = 0$. In Fig. 4 are also plotted the energy resolutions for all the points of the scan. A Gaussian fit to that distribution gives $\sigma = 2.0\%$.

The effect of the crack is small; a decrease of $\sim$ 7% is observed in the crack but not so localized as for the muon case: the signal decrease starts about 5 cm before the crack. In the same region in the corresponding plot for muons (fig. 2), the signal is still flat. The signal decrease starts before for pions as a result of the increased transverse dimension of the hadronic shower.

Figure 5 shows the energy spectra for 180 GeV pions at incident angle $\theta = 10circ$ in the center of module 3 and in the crack between modules 3 and 4. The effect of the crack is clearly visible by the shift of the distribution to lower energies ($\sim$ 7% smaller) and the development of a low energy tail resulting from the increased longitudinal leaking probability. The energy resolution increases from 1.5% in the central region to 2.4% in the crack using full fit region.

The signal response for 180 GeV pions as a function of the vertical displacement y for each of the four longitudinal compartments is shown in Fig. 6, separately for PMTs which readout the fibres near the crack, far from the crack, and for all the PMTs of modules 3 and 4. The signal behavior in the crack is very different from the muon response (see Fig. 3). For pions the signal in the crack is reduced to about 81% and 86% in depth 1 and 2, respectively. For depth 3 and 4 it is observed an increase of the signal of about 9% and 20% respectively. The explanation came from the fibres direct response (see section 6) and the increase of shower transverse dimension with depth. With the increase of the depth and the shower development a smaller part of the particle energy escape through the gap. As the interaction length is longer in the gap region, as it contains no iron, the shower has a broader longitudinal dimension and its peak moves to a larger depth, contributing to the increase of signal with depth in the crack region. This effect goes in the opposite direction of the increased longitudinal leakage probability. The signals sum for the 4 longitudinal compartments in the crack is only a 7% drop, as can be seen in Fig. 4, due to a cancellation effect which leads to an overall uniformity.

The plots obtained for other pion energies (20, 50, 100 and 300 GeV) are presented in Fig. 7. The uniformity is also good and the effect of the crack is small.

5 Energy resolution ϕ-scan at $\theta = 10^\circ$

A vertical scan was performed with pions with energies of 20, 50, 100, 180 and 300 GeV, between the center of module 3 and the center of module 4.

Peak and σ values were obtained from the raw energy spectra by Gaussian fits over a $\pm 2\sigma$ range. Fig. 8 shows the resulting σ/E as a function of $1/\sqrt{E}$ for two y impact positions, at the centre of module 3 ($y = -10cm$) and in the crack between two modules ($y = 0cm$).

Similar plots were done for different y positions to check for the response uniformity, the energy resolution and the effect of the crack. Each plot was fitted with the function

$$\frac{\sigma}{E} = \frac{a}{\sqrt{E}} + b \qquad .$$

Some of the fits are very bad, but in general the function describes reasonably well the experimental data. In figure 9 the distributions of parameters a and b are plotted as a function of y. These distributions have a reasonable uniformity inside the errors and the effect of the crack is not clearly visible. If a gaussian fit would have been done in all the energy spectra instead of a $\pm\sigma$ some degradation would be observed in the crack (see figure 5).

6 Muon scan at 90°

In this section are reported the results of a vertical scan with muons across the modules 3 and 4 lateral face ($\theta = 90°$), the y coordinate, for different depths, the z coordinate. In figure 10 is shown the experimental arrangement; the scan is done across the crack between the modules, with the muon beam perpendicular to this face (direction of the x axis). The signals on the PMTs reading the fibres passing through the crack between modules 3 and 4, of the cells corresponding to the first depth, S1, towers 2 to 5, of modules 3 and 4, were recorded. As the tower T1 is equiped with spliced fibers (scintilating fibers in the readout region, clear fibers outside this region) no direct fiber response is produced outside the tiles readout region and they are not considered in this study. The other towers are equiped with scintilating fibers with ultraviolet absorver (UVA) to decrease the direct fiber response due to Cherenkov light. This study allows to check the crack dimensions and to measure the direct fibre response.

Figure 11 shows the signal as a function of the y coordinate ($y = 0$ corresponds to the center of the crack) for a depth outside S1. As the tile is not traversed by the muon beam, it is clearly visible the peak corresponding to the direct fibre response, which is fitted with a gaussian. This peak goes well above the noise. Looking to the amplitude of the fibre direct response for different positions along the fibre and plotting it, the fibre attenuation length can be extracted (figure 12). In figure 13 it is shown the distance between the fibres in modules 3 and 4 (the distance between the peaks of fibre direct response) as a function of the fibre length which measures the crack dimension along the module.

Finally figure 14 shows the signal collected in one side of the crack, module 3, with the muons impinging in S1 where it is visible the tile response (about 4.5 pC) and the crack (signal decrease).

7 Conclusions

The analysis of the ϕ-scan data from the May 95 test beam period allowed to study the response uniformity and energy resolution from the center of module 3 to the center of module 4. The response uniformity is rather good ($\sigma = 2.0\%$ (2.4%) for 180 GeV pions (150 GeV muons)) and the effect of the crack between modules is limited to a small region. In the gap region the signal response decreases by about 7% (60%) for pions (muons). The energy resolution is also an uniform function of the y coordinate. A scan in the lateral face ($\theta = 90°$) across the crack allows to test the fibre direct response and the crack dimension. This study shows that the TILECAL uniformity, with the new tile geometry, masking and wrapping, is good.

References

[1] W.W. Armstrong et al., "ATLAS Technical Proposal for a general-purpose pp experiment at the large hadron collider at CERN", CERN/LHCC/94- 43, LHCC/P2, December 1994.

[2] F. Ariztizabal et al., NIM A349 (1994) 384.

[3] E. Berger et al., "Construction and performance of an iron-scintillator calorimeter with longitudinal tile configuration", RD-34 Collaboration, CERN-LHCC 95-44, LRDB status report/RD34, 1995.

[4] M. Bosman et al., "Study of the crack region between modules of the TILECAL prototype", unpublished TILECAL note, May 1994.

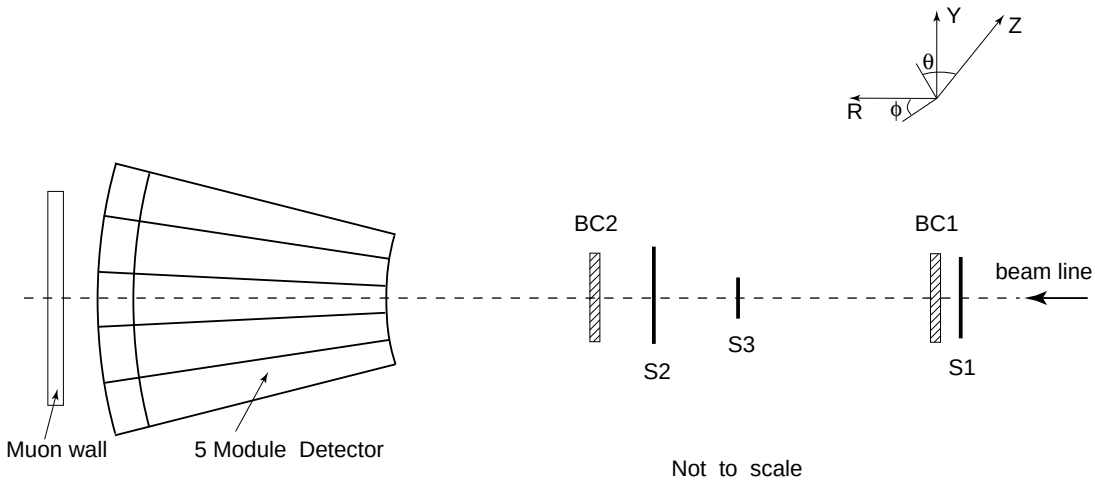

Figure 1: The arrangement of the five prototype modules in the beam line. The coordinate axis used are also shown.

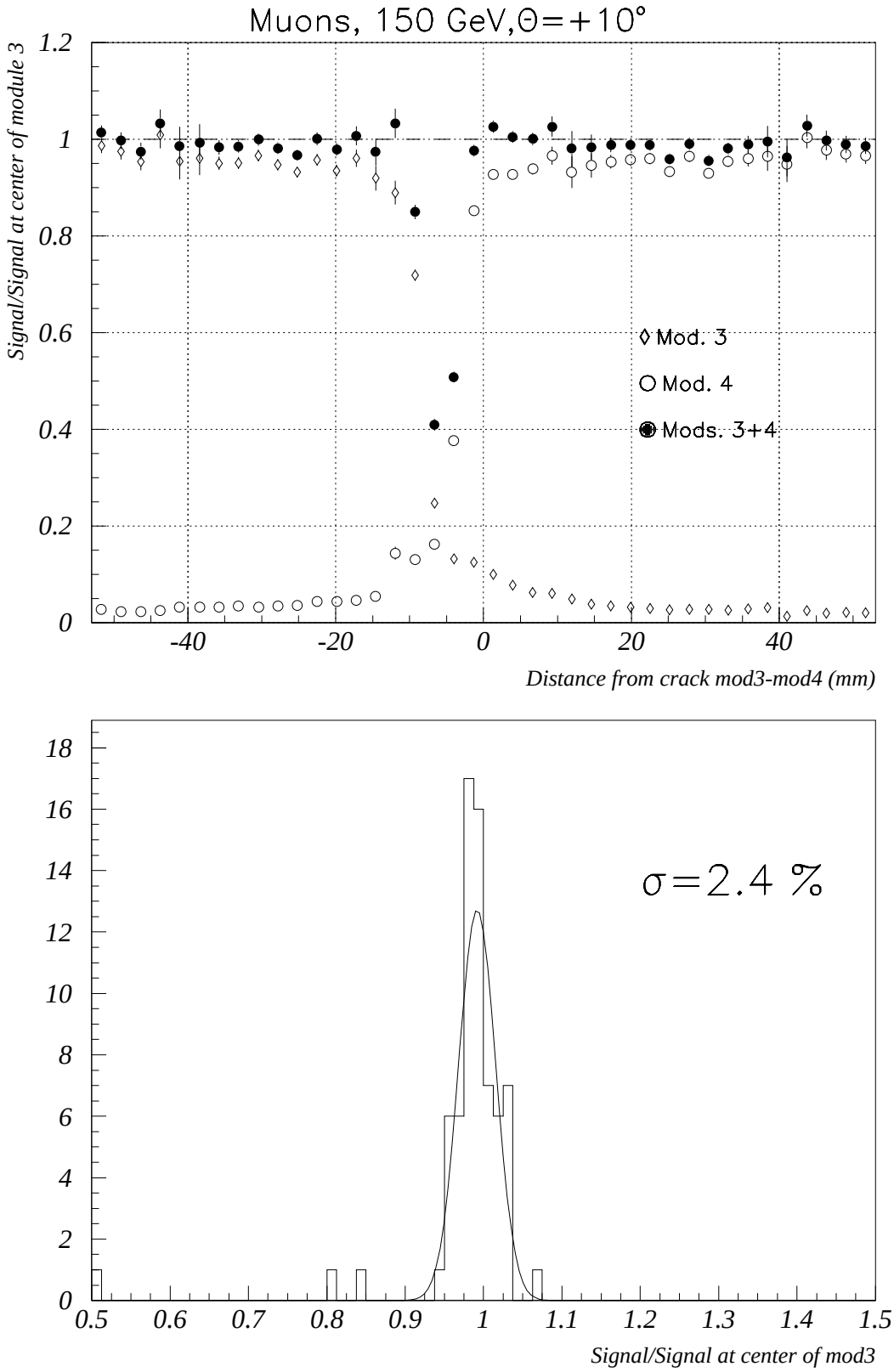

Figure 2: Top: Uniformity scan along the ϕ direction, obtained with 150 GeV muons impinging at $\theta = 10°$. Bottom: Normalized distribution of the most probable value of energy deposited by muons.

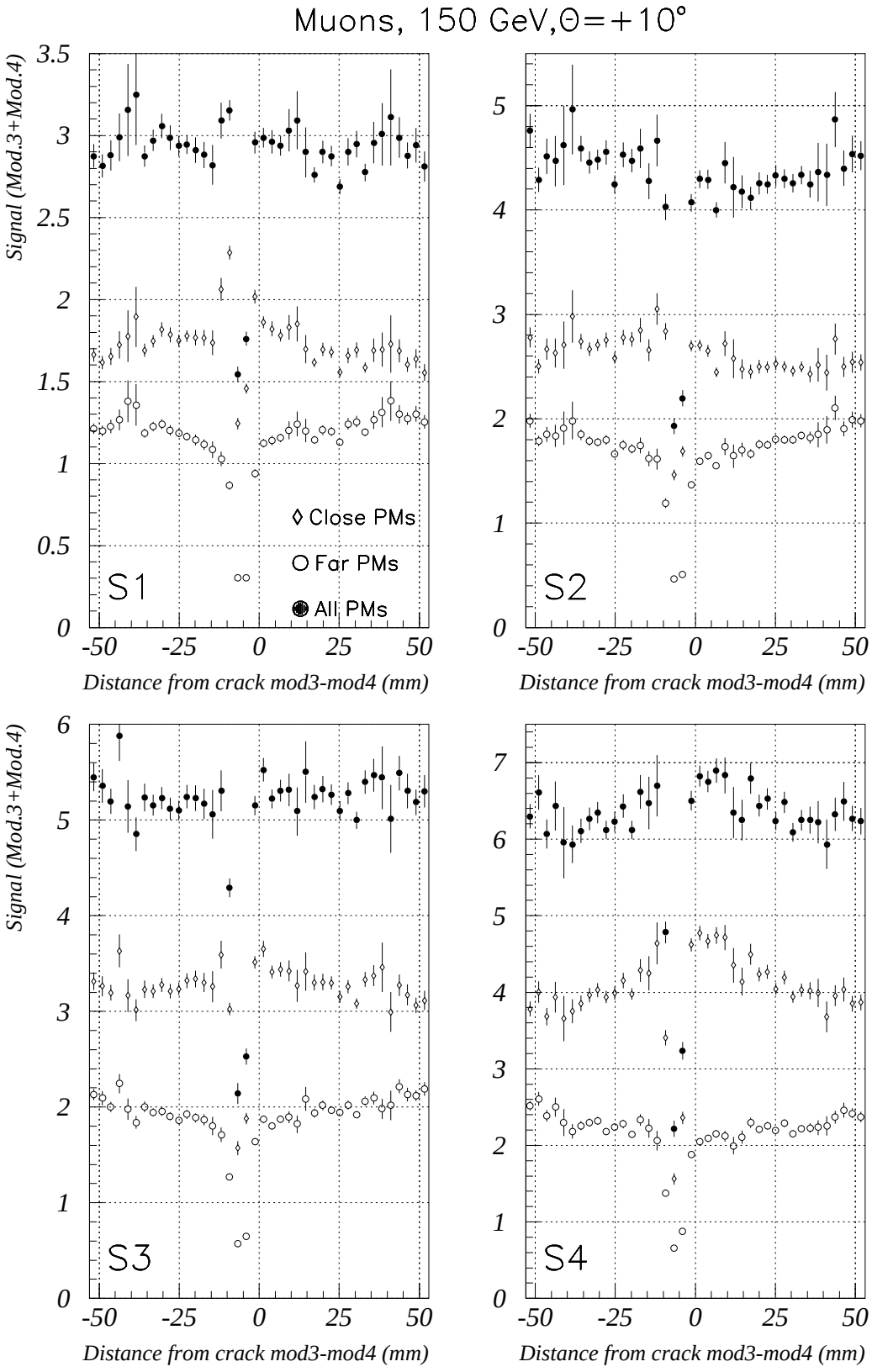

Figure 3: Uniformity of response along the ϕ direction for each of the four longitudinal compartments obtained with 150 GeV muons impinging at $\theta = 10°$.

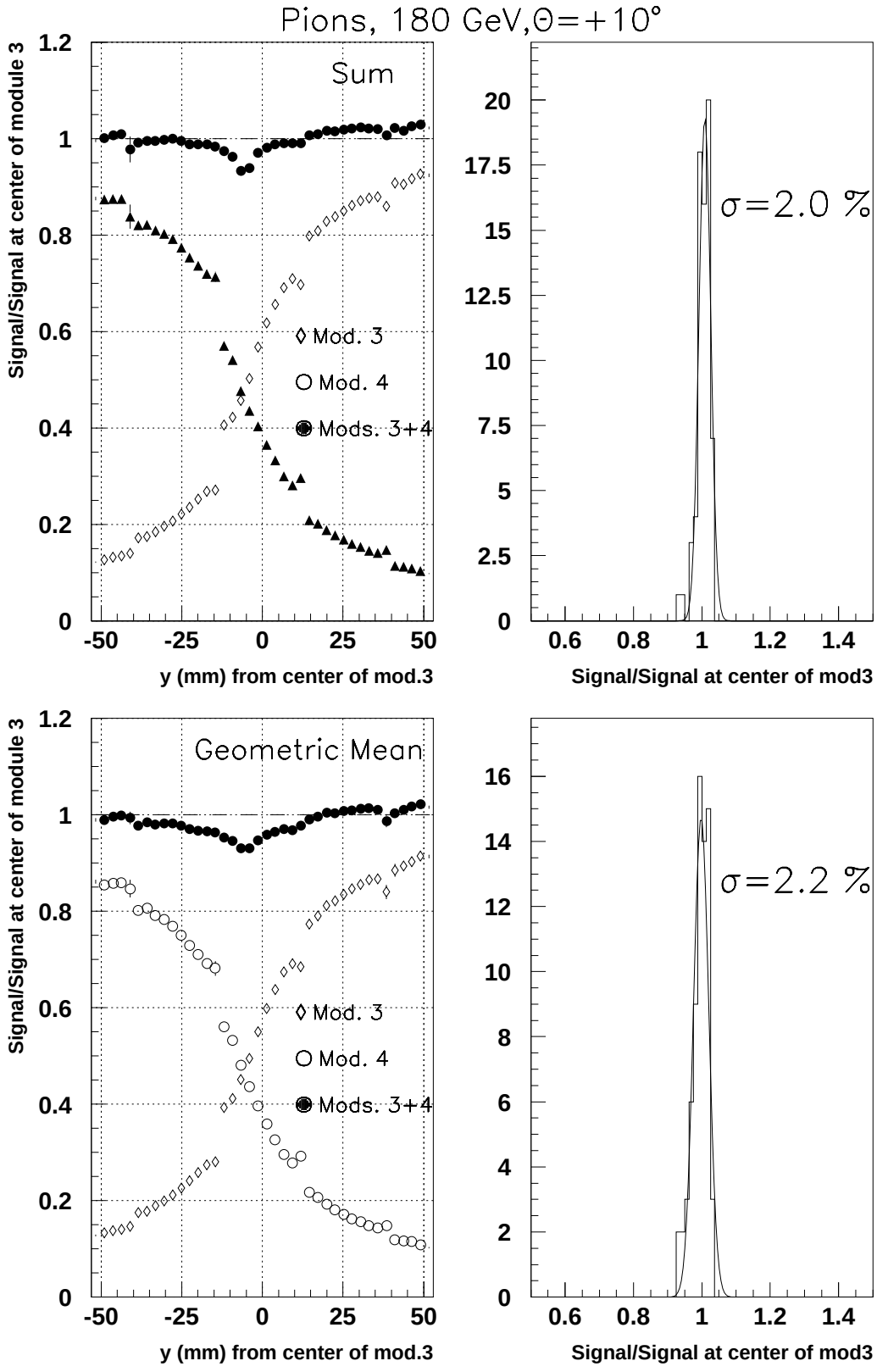

Figure 4: TOP - Left: Response of the calorimeter to 180 GeV pions as a function of the vertical coordinate y. The scan covers the region from the center of the central module (module 3) to the center of the upper module (module 4). Right: Projection of the peak values obtained in the grid scan fitted by a Gaussian. The values were normalized to the value at the center of module 3 and not to the average value. For this reason the distribution is not centered at 1. BOTTOM - The same thing but now using the geometric mean of the signals readout in the two sides of each cell.

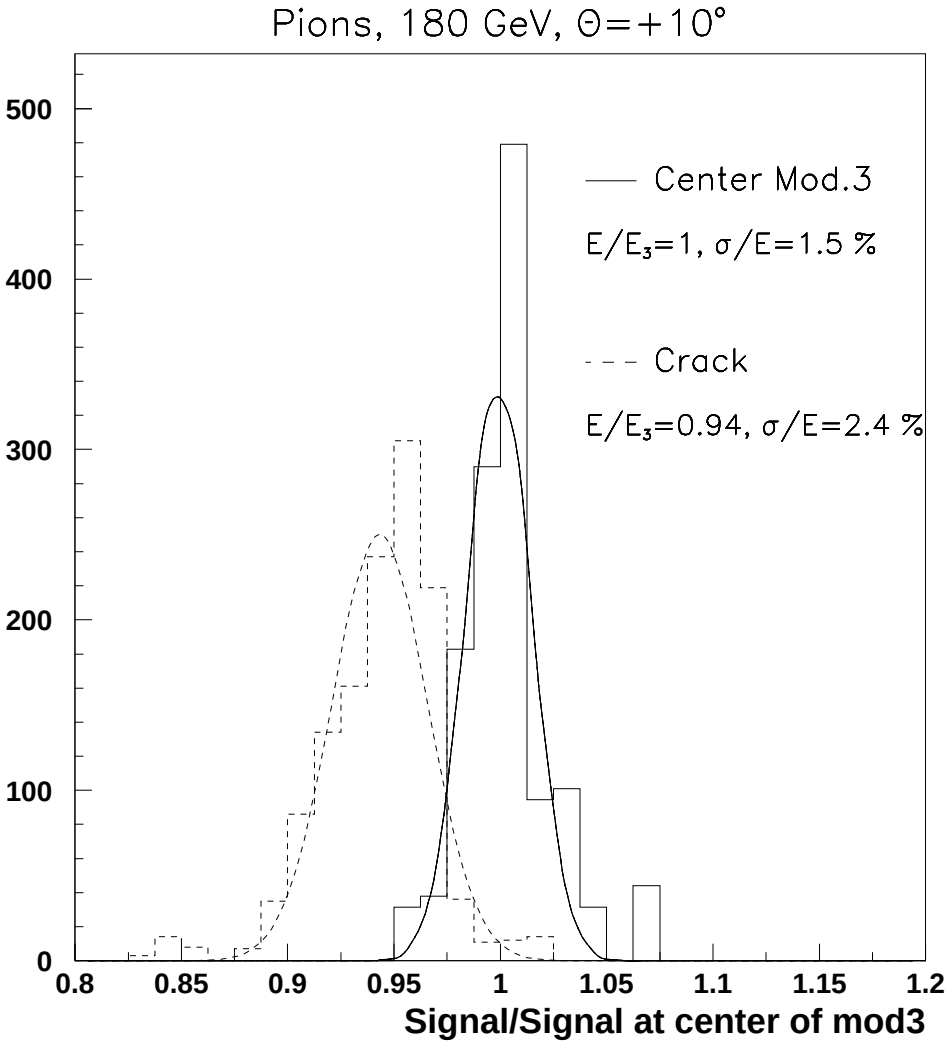

Figure 5: Distributions of energy deposited by the pion beam in the center of module 3 and at the crack. The effect of increased probability of longitudinal leaking in the crack is clearly visible by the shift of the spectrum and the low energy tail.

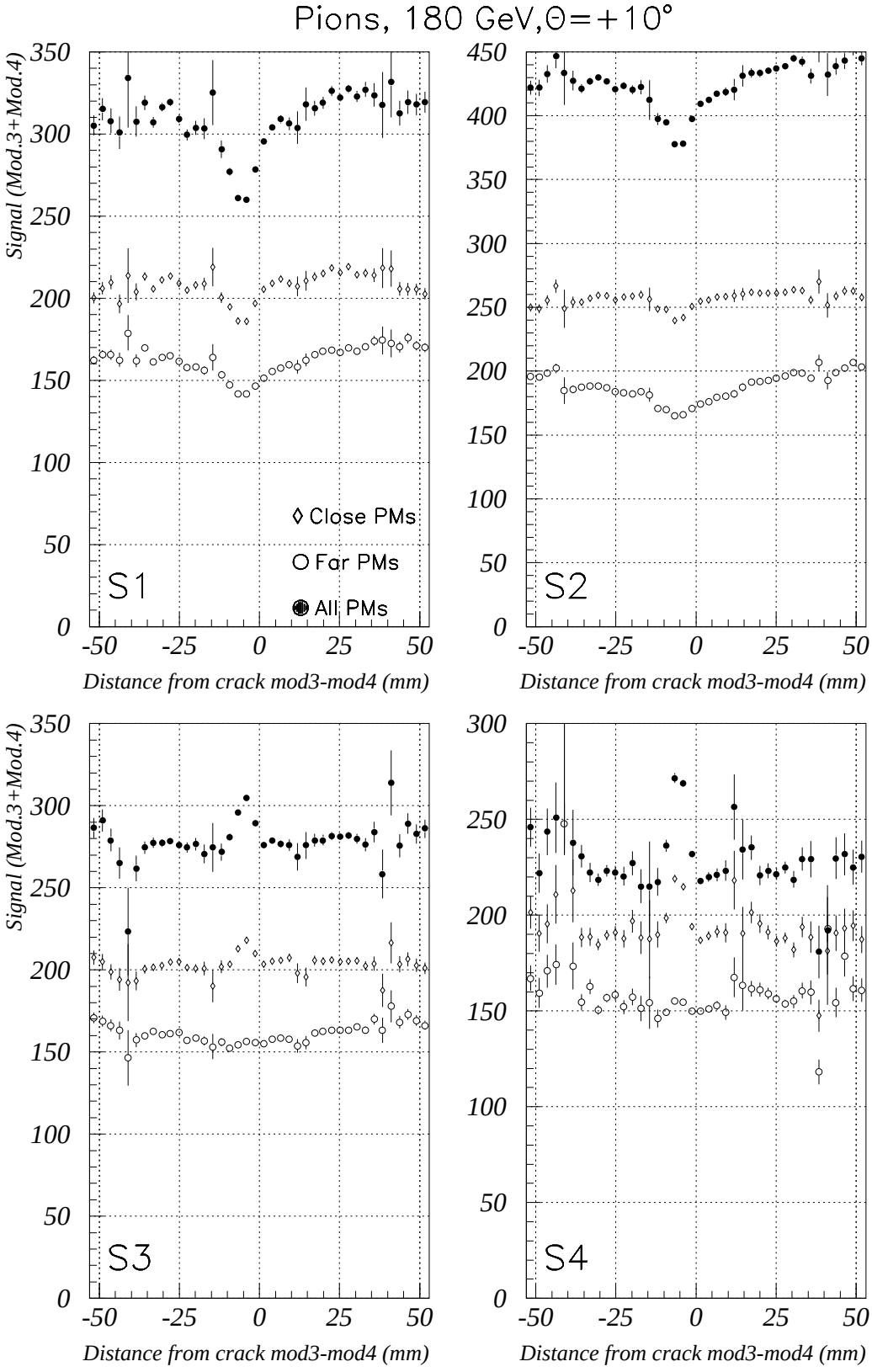

Figure 6: Uniformity of response for each of the four longitudinal compartments along the ϕ direction obtained with 180 GeV pions impinging at $\theta = 10°$.

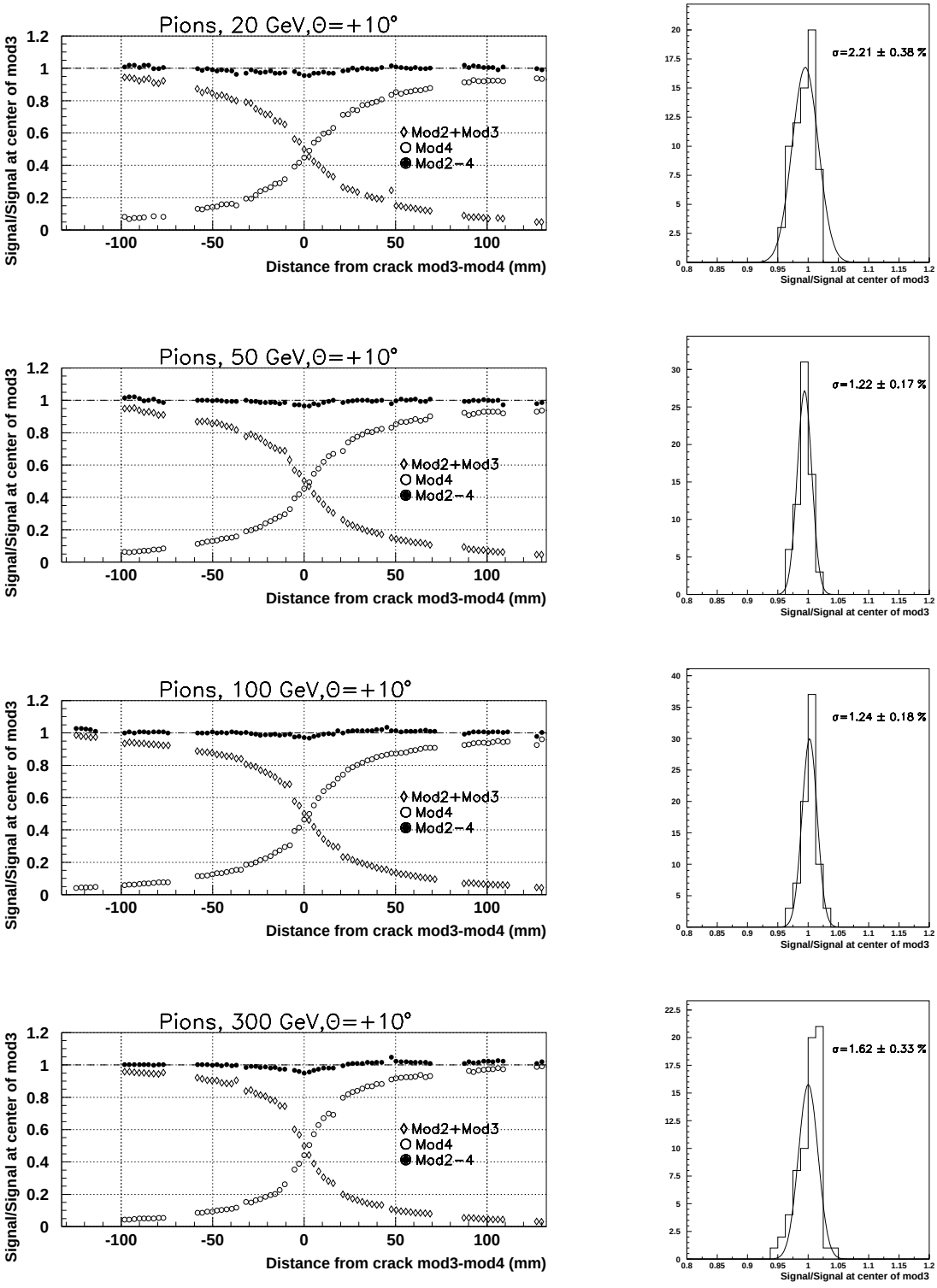

Figure 7: Left: Response of the calorimeter to pions as a function of the vertical coordinate y. Right: Projection of the peak values obtained in the grid scan, fitted by a Gaussian. The different rows correspond to different pion energies.

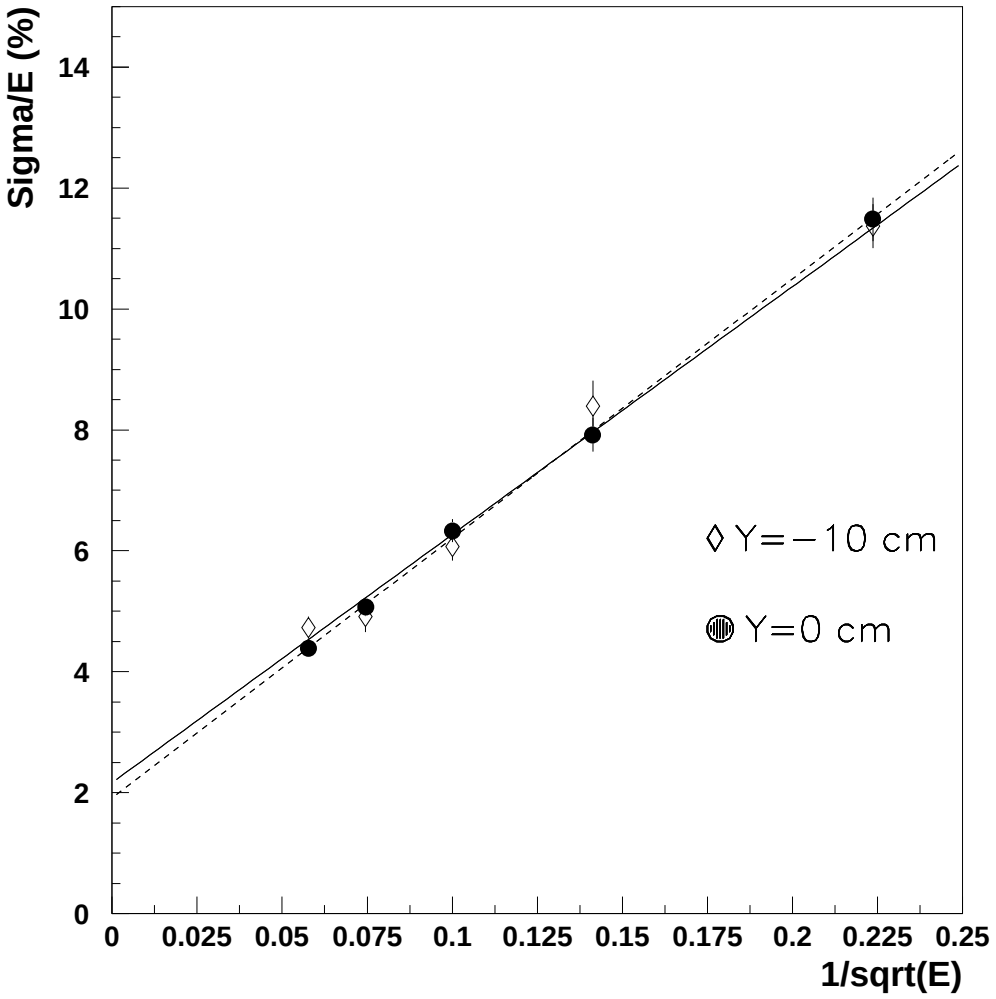

Figure 8: Energy resolution as a function of the energy for two different y bins.

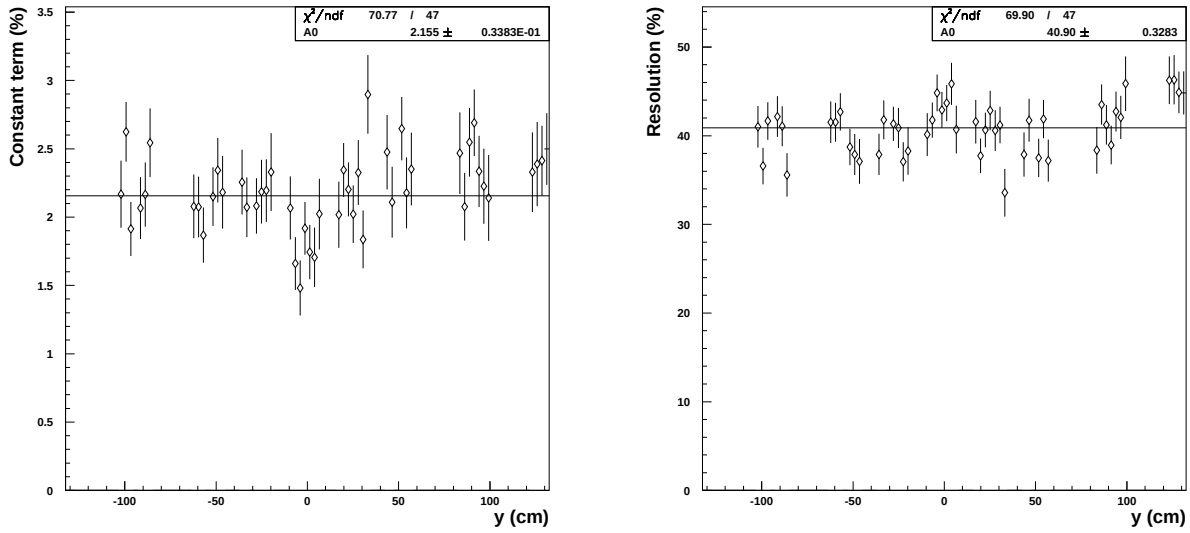

Figure 9: Left: Distribution of the parameter a from the energy resolution fit as a function of y. Right: The same for the parameter b. The crack is at $y = 0$ and the center of module 3(4) at -165(+165) cm.

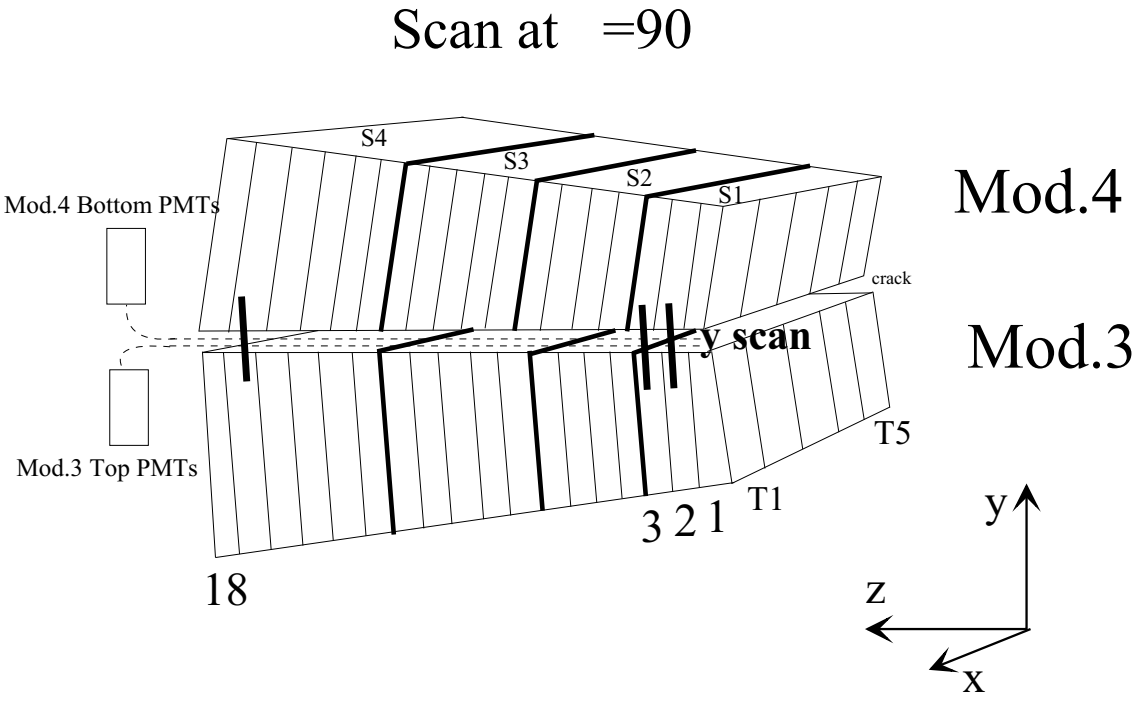

Figure 10: The arrangement used for the ϕ scan with muons at 90° across the crack between modules 3 and 4. Also shown are the coordinate axis used.

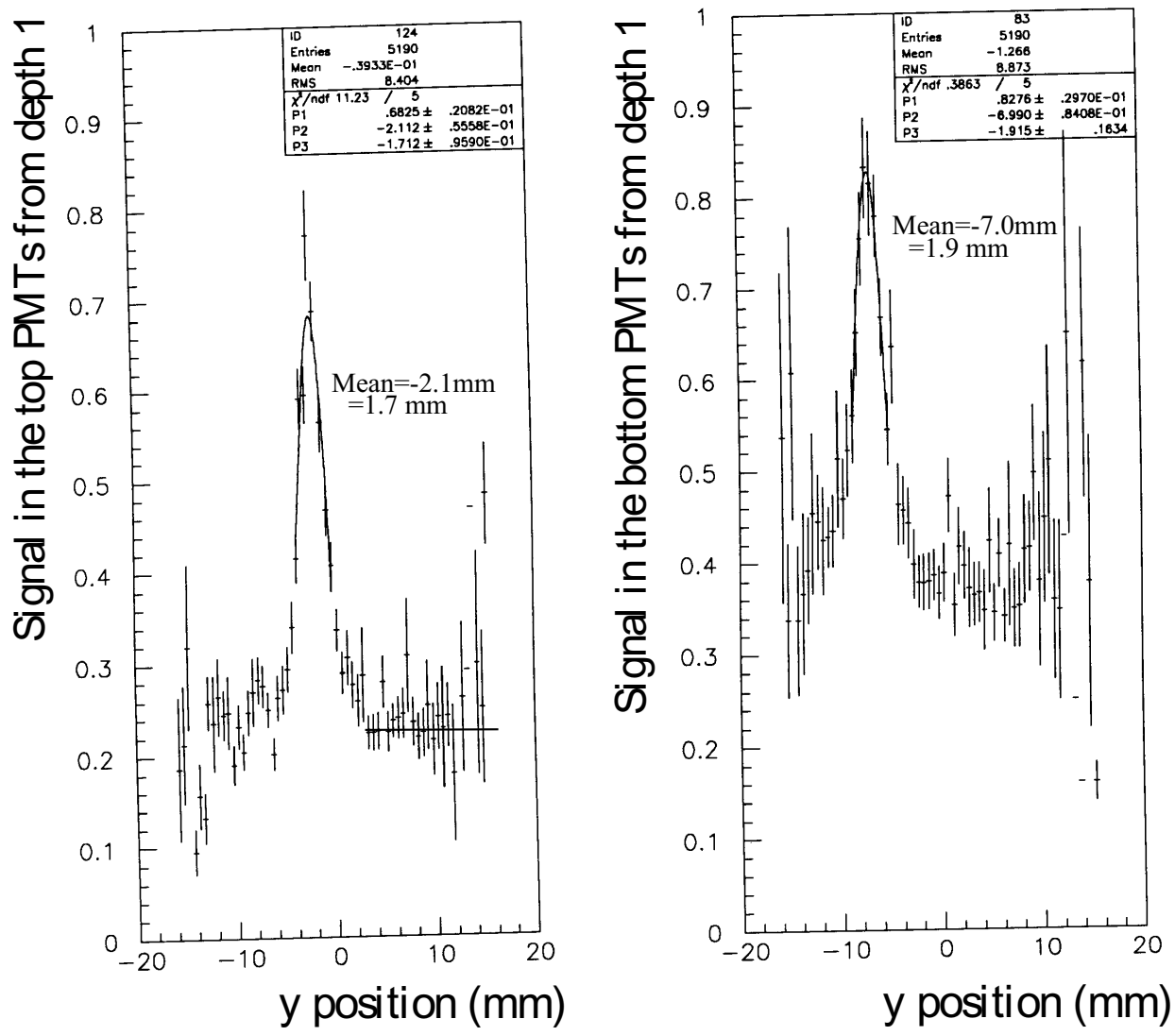

Figure 11: Signal in depth 1, towers 2 to 5, as a function of the vertical coordinate along the modules lateral face, for a scan across the crack outside depth 1. The peak is due to the direct fibre response and it is fitted by a gaussian.

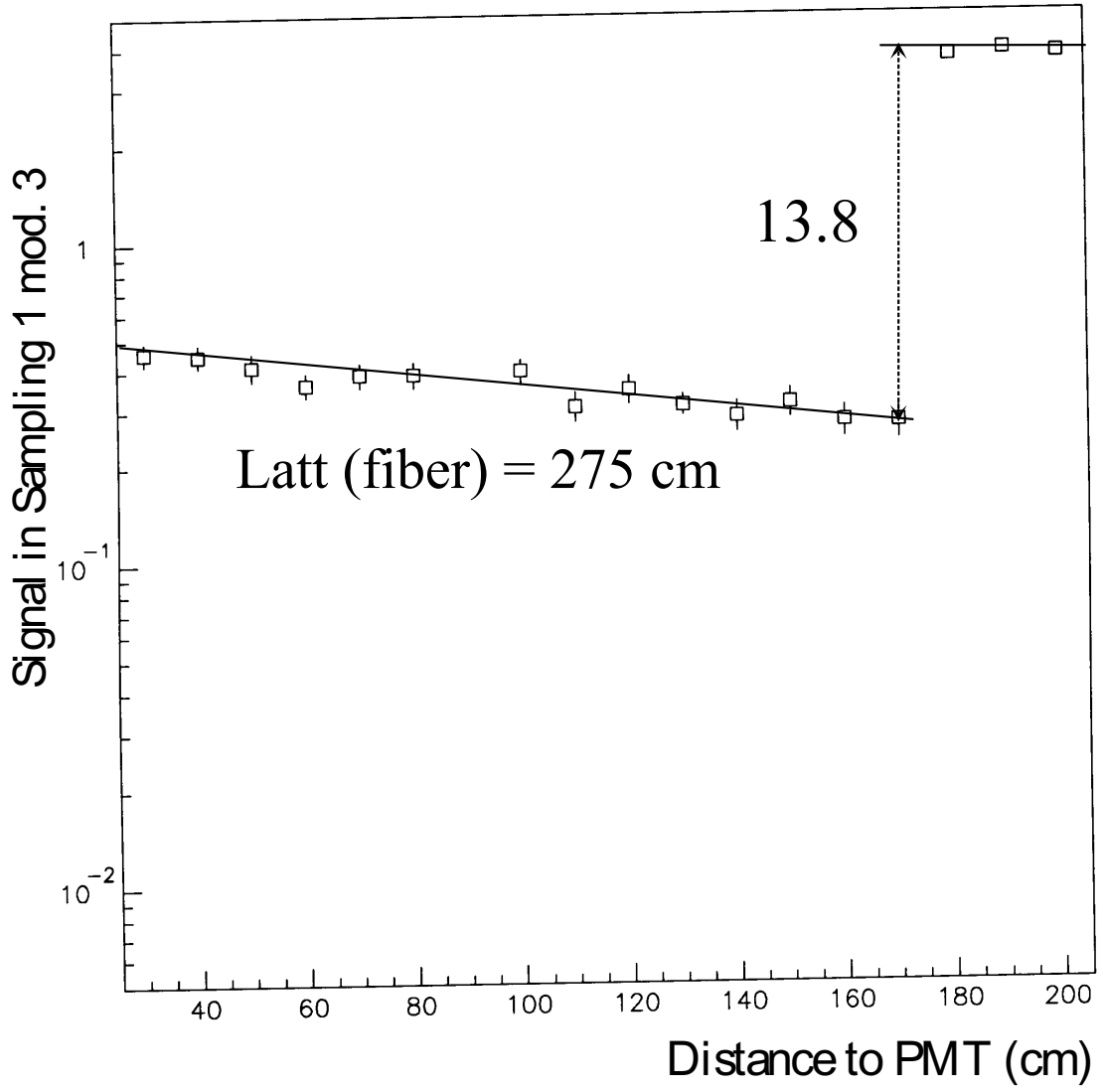

Figure 12: Signal in sampling 1 as a function of the distance along the module. From the direct fibre response can be extracted the fibre attenuation length.

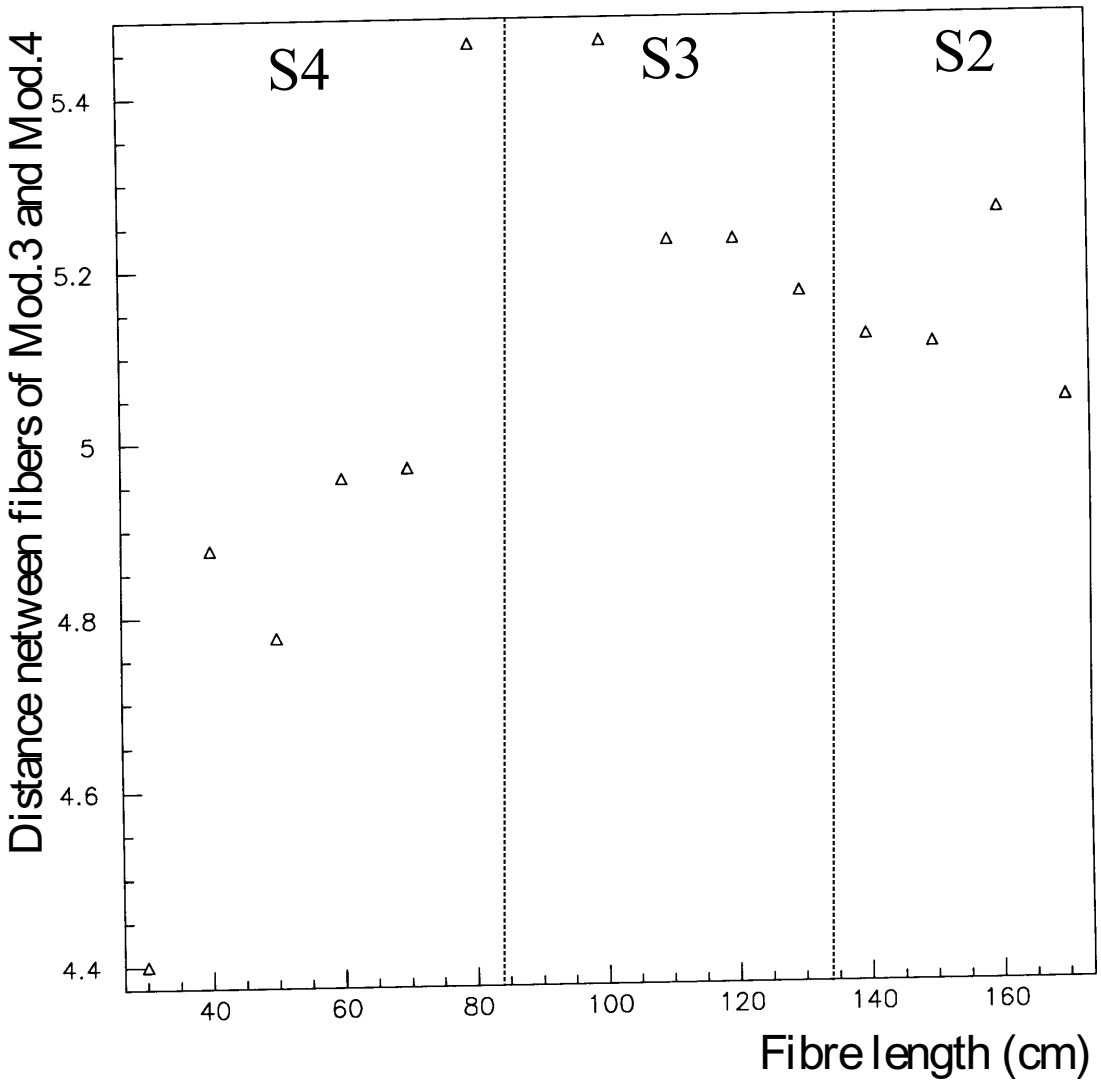

Figure 13: Distance between the fibres of modules 3 and 4, the crack dimension, as a function of the fibre length.

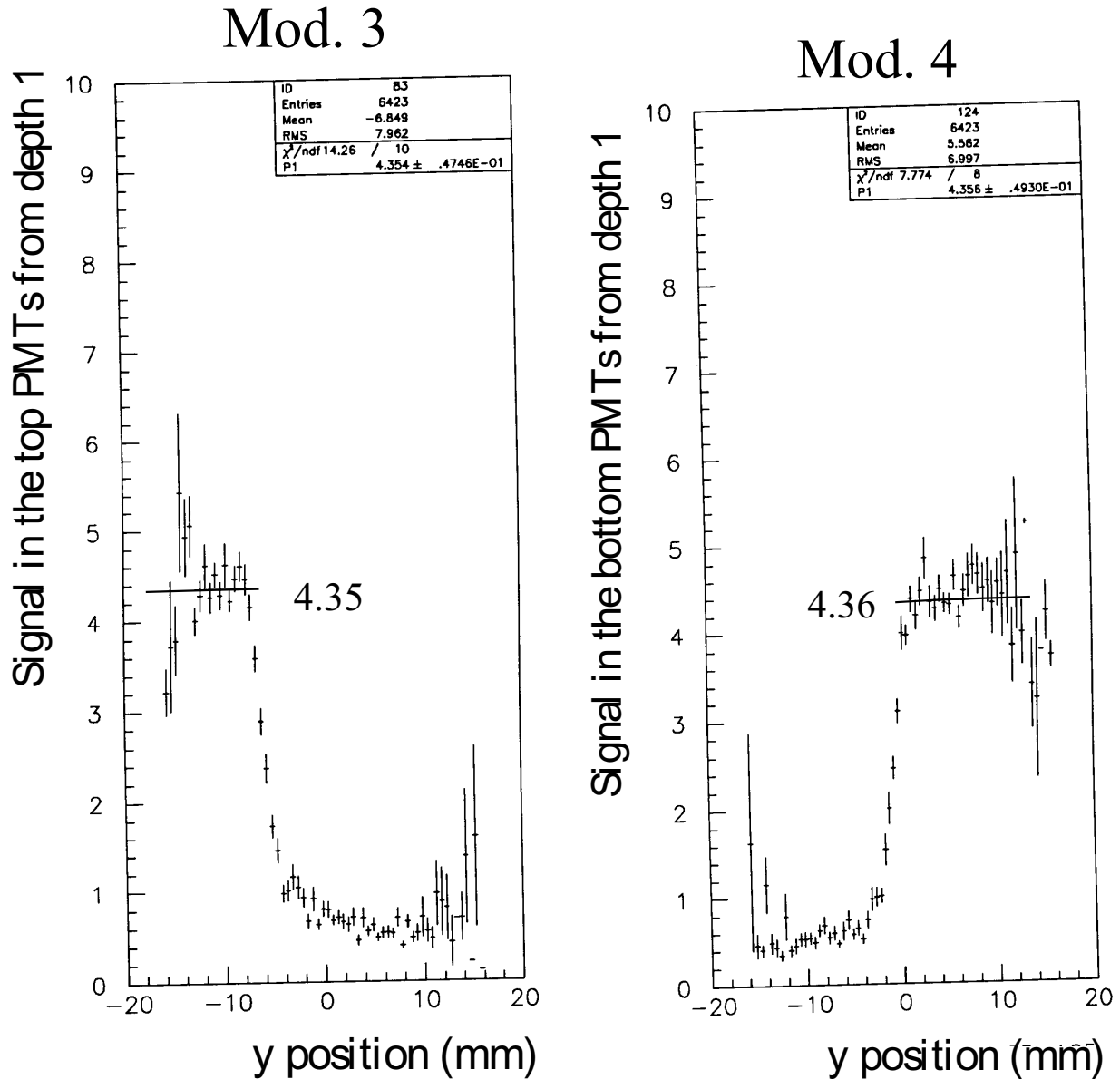

Figure 14: Scan across the crack at depth 1. It can be seen the tile response and the crack position.